Hybrid Late Fusion for UAV RGB Soybean Disease Detection and Spray Decision Support

Kishan Kumar Yadav[1], Aruna Tiwari[1], Rajesh Dwivedi[2], Pavan Kumar Kankar[1],
Satya Prakash Kumar[3], Shashi Rawat[3], and Milind Ratnaparkhe[4]
[1]Indian Institute of Technology Indore, India
[2]Indian Institute of Information Technology, Ranchi, India
[3]ICAR–Central Institute of Agricultural Engineering, Bhopal, India
[4]ICAR–National Soybean Research Institute, Indore, India

***Abstract*—Low-cost UAV RGB imagery provides a practical solution for large area soybean health monitoring, but disease detection remains difficult due to class imbalance, background clutter, and illumination variation. To address these challenges, we propose a hybrid late fusion framework that combines an EfficientNet B3 image encoder with lightweight, interpretable numeric cues derived from each canopy tile, including vegetation color statistics, brightness and blur measures, and a leaf-area prior. The model is trained using imbalance aware learning to reduce bias towards majority classes. Experiments conducted on 2,842 UAV canopy tiles across four classes, i.e., Healthy, Mosaic, PestAttack, and Rust show that fusion improves robustness and achieves a test macro-F1 of 0.98, with strong per class F1 scores (0.99/0.97/0.98/0.97). Beyond disease recognition, we introduce an RGB only severity proxy based on leaf masking and class-specific color and texture cues. This enables an action-oriented decision policy that outputs *SPRAY*, *MONITOR*, or *NO SPRAY*, along with pixel-level overlays to enhance interpretability. Using conservative thresholds, the system achieves *a SPRAY* precision of 1.00 and a recall of 0.83 on the test set. Precision recall analysis reveals that recall can be increased with minimal loss in precision. The proposed RGB only pipeline, in general, provides a comprehensive path from UAV based disease detection to practical spray decision support for precision crop protection.**

***Index Terms*—UAV imagery, soybean disease, late fusion, EfficientNet, vegetation indices, severity estimation, spray decision support**

I. Introduction

Soybean is a globally important oilseed crop, providing edible oil and protein rich meal for human consumption and livestock feed [1]. Despite its economic importance, soybean production is persistently threatened by diseases and pest infestations. Historical assessments report that global soybean yield losses due to diseases alone increased from $\sim$11% in 1994 to nearly 27% by 2006 [1]. Such losses reduce farm profitability and have an impact on food security and supply chain stability, emphasizing the importance of timely and accurate disease detection.

Traditional diagnosis relies on manual scouting and laboratory procedures, which are labor intensive, time consuming, and prone to subjectivity when symptoms are subtle or spatially heterogeneous. In addition, for large fields, frequent ground inspection is impractical, necessitating remote sensing solutions that scale to the field level. Unmanned aerial vehicles (UAVs) are gaining popularity in precision agriculture due to their ability to capture high-resolution imagery with flexible deployment and low operational costs [2]. Early UAV studies emphasized spectral index-driven monitoring using multispectral/hyperspectral sensors, enabling early stress detection beyond visible cues [3]. However, such sensing increases system cost, payload, and calibration complexity, motivating RGB only alternatives that are cheaper and easier to deploy at scale [2], [4]. Deep learning has significantly advanced image-based plant disease recognition, initially driven by large-scale leaf-image benchmarks [5], [6] and later extended to soybean-specific recognition in realistic settings. UAV based soybean disease recognition with RGB imagery has shown strong potential using transfer learning and Convolutional Neural Network(CNN) backbones [7], and related UAV/field pipelines address pests and canopy variability [8]. Recent lightweight and transformer-based models support deployable plant disease recognition under constrained compute.

Nonetheless, disease detection through UAV RGB remains challenging in real field conditions: canopy tiles often mix healthy and stressed plants, symptoms can be sparse, and illumination/background vary across flights. Although large frames are tiled for CNN inference, tile-level predictions may not reflect the larger region, yielding biased aggregation and unstable recommendations [7]. Moreover, classification alone is insufficient for farm decisions; practical spraying requires reliable predictions along with an estimate of disease extent/severity, motivating conservative, action-oriented policies [9], [10].

Based on these considerations, we propose a hybrid late-fusion framework for soybean disease detection and spray decision support using only UAV RGB imagery captured by a compact DJI Mini 4 Pro drone. The proposed system focuses on four agronomically significant canopy health categories: *Healthy*, *Mosaic*, *PestAttack*, and *Rust*. Our method combines deep visual representations extracted using an EfficientNet-B3 CNN backbone [11] with lightweight, interpretable numeric indices derived from RGB imagery. These indices encode domain knowledge related to vegetation vigor, texture, and canopy structure (e.g., color/vegetation indices and texture statistics) [12]–[14]. The heterogeneous cues are fused in a late-fusion architecture to improve robustness in the presence of canopy heterogeneity while maintaining interpretability. Disease recognition is only valuable if it enables reliable intervention: false sprays waste chemicals and cost, while missed detections can cause severe yield loss. Although UAV RGB imagery is low-cost and scalable [2], tile-based CNN predictions can be unstable when symptoms are sparse; therefore, we fuse CNN embeddings with lightweight agronomic numeric cues and use a severity-aware decision policy that converts confidence and estimated extent into actionable recommendations (*spray/monitor/no action*) for robust and interpretable UAV based crop monitoring [7], [12], [13]. The dataset used in this work is publicly available DOI: 10.17632/hkbgh5s3b7.1 (direct link). [8].

II. Related Work

UAV enabled crop monitoring has become a practical alternative to labor-intensive field scouting because it provides high-resolution, field-scale imagery with flexible acquisition and rapid coverage [2]. Table I summarizes representative UAV/field studies and approaches used in that studies. Early disease and stress studies often relied on multispectral or hyperspectral sensing to capture physiological changes that may not be visible in RGB. For example, [3] used UAV hyperspectral imagery with feature selection and an SVM classifier to detect powdery mildew in squash across disease stages, reporting strong performance. While such spectral pipelines can be sensitive to early stress, they typically increase system cost and introduce calibration/payload overhead, limiting routine deployment for many farms.

To improve deployability, several works have explored RGB only pipelines on UAV or field imagery. In soybean, [15] applied SLIC superpixels with handcrafted color/texture/shape descriptors and classical classifiers, achieving high precision under controlled acquisition settings. However, handcrafted pipelines can be brittle under illumination shifts, background clutter, and canopy heterogeneity, which are common in UAV flights. Moving toward deep learning, [7] used transfer learning with a ResNet-101 backbone on UAV RGB soybean imagery and achieved high recognition accuracy. Despite strong results, RGB only CNN classifiers can still be affected by mixed tiles (healthy and diseased regions in the same view), class imbalance, and background intrusion, which can reduce reliability when predictions must support field actions.

Pest recognition from RGB field imagery has also been studied in soybean. In [16], fine-tuned CNN backbones were used for pest-related classification, demonstrating that deep models can capture discriminative cues under field conditions. A practical limitation is that pest damage is frequently sparse and localized; therefore, patch-level predictions may not reflect actionable severity at field scale, and confidence alone may not be sufficient for intervention planning.

Beyond soybean, RGB disease detection and localization has been explored for other crops. In [17], a YOLOv7-based real-time detector was proposed for tea leaf disease identification, and [18] improved disease detection using an attention-enhanced RetinaNet variant. While detection frameworks support real-time localization, they often treat symptom presence as directly actionable; in practice, intervention decisions require an estimate of extent/severity and conservative control to avoid unnecessary spraying.

Studies in wheat further illustrate modality and task trade-offs. In [4], UAV RGB imagery was compared against hyperspectral data for wheat monitoring, showing hyperspectral advantages but with higher sensing and operational complexity. For spatial disease mapping, [19] used UAV multispectral imagery with an improved U-Net (Ir-UNet) for wheat rust segmentation, enabling area-level delineation. Although segmentation is well-suited to quantify affected area, it often requires pixel-level annotations or careful weak/assisted supervision and can be harder to scale across new sites and seasons. RGB only UAV mapping has also been explored with lightweight deep models; [20] reported strong macro-F1 for downy mildew detection and field mapping in cabbage while emphasizing efficiency, though robustness across illumination/canopy density shifts remains a practical challenge. Hybrid deep-feature+ML approaches have also been reported for multi-disease recognition in UAV wheat imagery [21], but such systems may still inherit sensitivity to flight variation and do not necessarily address action reliability under mixed canopies.

An increasingly important direction in precision agriculture is decision-oriented monitoring, where perception outputs are translated into field interventions. In [10], a deep-learning-based variable-rate spraying strategy was evaluated in field conditions and reported substantial spray savings. This highlights that action policies matter as much as recognition accuracy: overly aggressive triggers can cause over-spraying, whereas overly conservative ones may miss early infestations. However, many existing pipelines still rely on heuristic thresholds or do not explicitly combine uncertainty (confidence) with estimated extent (severity), making action behavior difficult to tune under asymmetric risk. Overall, prior studies demonstrate strong progress in UAV and field based disease monitoring, but they also reveal two practical gaps for low cost UAV RGB deployment: robustness under real flight variation, and the translation of recognition outputs into conservative, interpretable spray recommendations. Our method addresses these gaps through an RGB only hybrid late-fusion classifier, combining EfficientNet-B3 embeddings with lightweight numeric cues, together with a severity aware decision policy that produces SPRAY, MONITOR, or NO-SPRAY recommendations.

III. Methodology

The proposed framework in Fig.1 is designed with the primary objective of achieving reliable soybean disease detection and actionable spray decision support using only UAV RGB imagery. Each component of the methodology is motivated by practical constraints encountered in real-world field deployment, including limited sensing modalities, class imbalance, and the spatial sparsity of disease symptoms. This

TABLE I: Comparison of Related Works for Crop Disease Detection

Study	Year	Dataset	Approach	Reported Metric
Mahmood *et al.* [21]	2026	UAV imagery (wheat)	VGG-16 features + ML classifiers (multi-disease detection)	Acc: 97%, F1: 96%
Lyu *et al.* [20]	2025	UAV RGB (cabbage field)	Lightweight DL models for downy mildew detection and field mapping	Best Macro-F1: 0.918
Farooque *et al.* [10]	2023	Field RGB (potato)	Deep-learning-based *variable-rate* spraying evaluation	47–51% spray savings
Soeb *et al.* [17]	2023	Ground RGB (tea leaves)	YOLOv7-based real-time detector (YOLO-T)	Acc: 96.3%
Feng *et al.* [4]	2022	UAV RGB vs hyperspectral (wheat)	CNN-based comparison of sensing modalities for crop monitoring	Acc: 88.3% (RGB), 93.5% (Hyper)
Bao *et al.* [18]	2022	Ground RGB (tea leaves)	AX-RetinaNet for disease detection	mAP: 93.83%, F1: 0.954
Zhang *et al.* [19]	2021	UAV multispectral (wheat)	Ir-UNet segmentation for yellow rust mapping	Acc: ≈97%
Tetila *et al.* [7]	2020	UAV RGB (soybean)	Transfer learning with ResNet-101 (soybean leaf disease recognition)	Acc: 94.0%
Tetila *et al.* [16]	2020	Field RGB (soybean pests)	CNN-based pest classification from field imagery (fine-tuned backbones)	High accuracy (model-dependent)
Abdulridha *et al.* [3]	2020	UAV hyperspectral (squash)	Hyperspectral feature selection + SVM (powdery mildew detection at stages)	Acc: 95.76%, F1: 0.87
Tetila *et al.* [15]	2017	UAV RGB (soybean)	SLIC + hand-crafted color/texture/shape features + classical classifiers (foliar disease identification)	Precision up to 98.34% (low height)
Proposed hybrid late fusion	**2026**	UAV RGB (DJI Mini 4 Pro), soybean canopy	Hybrid late fusion (EfficientNet-B3 + RGB numeric indices) + confidence/severity-aware spray policy	Macro F1: **98.6%**

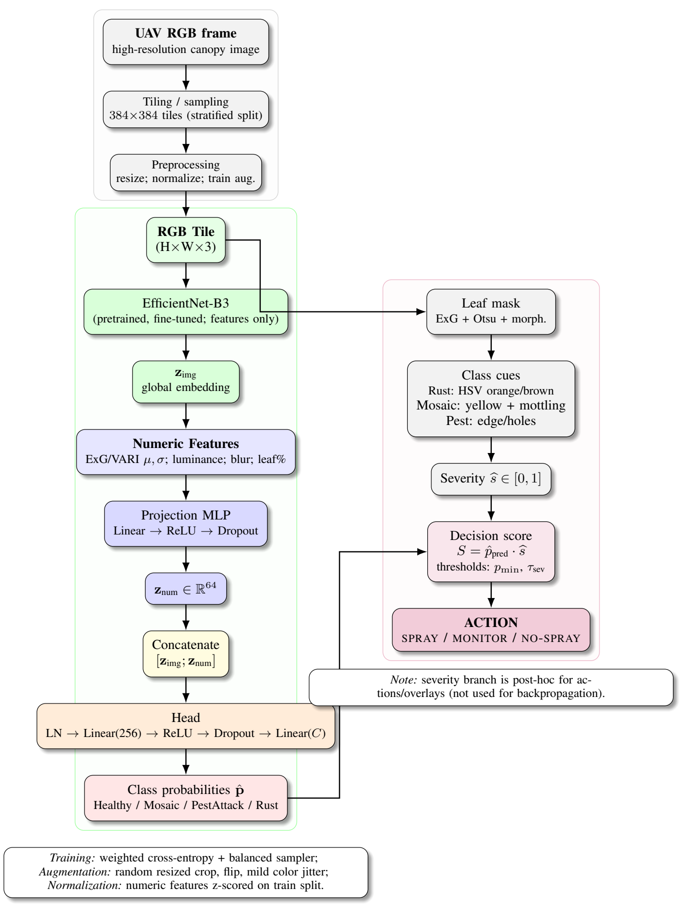

Fig. 1: Overview of the proposed hybrid late-fusion framework for UAV RGB soybean disease detection and spray decision support.

section details the dataset preparation, feature design, hybrid late-fusion architecture, training strategy, and decision-support mechanism, along with the rationale behind each design choice.

A. Dataset, preprocessing, and numeric cues

UAV imagery captures large canopy regions in which disease symptoms are often sparse and spatially localized. To reduce scale ambiguity while preserving local disease evidence, each UAV frame is partitioned into fixed-size tiles that serve as the basic learning unit.

We use the public MH-SoyaHealthVision dataset [8], which includes both handheld leaf images and UAV RGB canopy imagery annotated into four agronomically relevant classes: *Healthy*, *Mosaic*, *PestAttack*, and *Rust*. Fig. 2 summarizes the class distribution for the UAV subset. Unless stated otherwise, all quantitative results are reported on the UAV tile benchmark (N=2,842), where tiles are divided into train/validation/test sets using stratified sampling to preserve class proportions.

Each tile is resized and center-cropped to 384×384 pixels and normalized to $[0, 1]$; the test set uses only resize and crop to avoid optimistic evaluation. In addition to CNN-based image features, we compute lightweight numeric cues to capture color, illumination, focus, and canopy extent. Specifically, Excess Green (ExG) is computed as

$$\text{ExG} = 2G - R - B,$$

and the Visible Atmospherically Resistant Index (VARI) is computed as

$$\text{VARI} = \frac{G - R}{G + R - B + \epsilon},$$

where R, G, and B denote the red, green, and blue channel intensities, and ϵ is a small constant for numerical stability. We also compute mean luminance from the grayscale tile, blur using the variance of the Laplacian,

$$\text{Blur} = \text{Var}\left(\nabla^2 I\right),$$

and a leaf-area estimate obtained by applying Otsu thresholding to the ExG map followed by morphological cleanup. All numeric features are standardized using z-score normalization with statistics computed from the training split only.

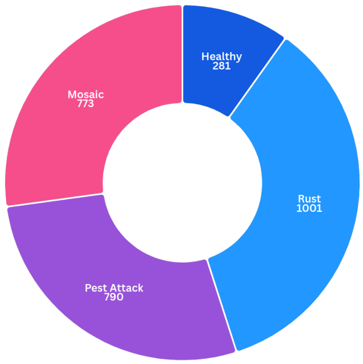

Fig. 2: Class distribution of the UAV tile benchmark across *Healthy*, *Mosaic*, *PestAttack*, and *Rust*.

B. Hybrid late-fusion model and training

The hybrid model is designed to combine the representational power of deep CNN features with the robustness and interpretability of lightweight numeric cues. This late-fusion strategy allows each modality to capture complementary information while avoiding interference during early feature learning.

Given an RGB tile $\mathbf{x}_{\text{img}}$ and its corresponding numeric vector $\mathbf{x}_{\text{num}}$, an EfficientNet-B3 backbone f_θ (ImageNet pretrained and fine-tuned) extracts a global visual embedding $\mathbf{z}_{\text{img}}$. In parallel, numeric cues are projected through a lightweight MLP to obtain $\mathbf{z}_{\text{num}} \in \mathbb{R}^{64}$. The two embeddings are concatenated and passed through a shallow classification head to produce class probabilities $\hat{\mathbf{p}}$.

UAV disease datasets are inherently imbalanced, with healthy tiles dominating the distribution. To mitigate bias toward majority classes and improve minority-class recall, we train the model using weighted cross-entropy together with a weighted random sampler.

C. Spray decision module and evaluation

In practical farming scenarios, disease classification alone is insufficient; actionable decisions must account for both confidence and estimated disease extent. To bridge this gap, we introduce a severity-aware spray decision module that converts recognition outputs into conservative field actions.

For each tile, we estimate an RGB only severity proxy $\widehat{s} \in [0, 1]$ representing the fraction of affected leaf area. A leaf mask is obtained using ExG, Otsu thresholding, and morphology, within which class-specific cues are activated (Rust: orange/brown HSV regions; Mosaic: yellow/light-green mottling with elevated local variance; PestAttack: leaf-loss and edge-density patterns). We then define an action score $S = \hat{p}_{\text{pred}}\widehat{s}$, combining model confidence with estimated severity.

Using per-class confidence ($p_{\min}$) and severity (τ_{sev}) thresholds, the system outputs SPRAY, MONITOR, or NO-SPRAY. This conservative policy prioritizes high precision to avoid unnecessary chemical application while allowing recall to be tuned based on operational risk.

Algorithm 1: RGB tile $\rightarrow$ action (4-step)

Input: tile I, numeric $\mathbf{x}_{\text{num}}$, thresholds $p_{\min}[c], \tau_{\text{sev}}[c]$
Output: $\hat{c}, \hat{p}, \widehat{s}$, action
$(\hat{c}, \hat{p}) \leftarrow \text{FusionNet}(I, \mathbf{x}_{\text{num}})$
if $\hat{c}$=*Healthy* ***or*** $\hat{p} < p_{\min}[\hat{c}]$ **then**
  return $\hat{c}, \hat{p}, 0,$ NO-SPRAY
$\widehat{s} \leftarrow \text{SeverityProxy}(I, \hat{c})$
action $\leftarrow$ **if** $\widehat{s} \geq \tau_{sev}[\hat{c}]$ **then**
  SPRAY
else
  MONITOR

Algorithm 2: Validation threshold tuning (4-step)

Input: validation set, grids $\mathcal{P}, \mathcal{T}$
Output: best $p_{\min}[c], \tau_{\text{sev}}[c]$
foreach $c \in \{Mosaic, PestAttack, Rust\}$ **do**
  sweep $(p, \tau) \in \mathcal{P} \times \mathcal{T}$ using Algorithm 1
  compute SPRAY F1 (diseased vs. healthy)
  select (p, τ) maximizing F1 and set
  $p_{\min}[c] \leftarrow p,\ \tau_{\text{sev}}[c] \leftarrow \tau$

IV. Results and Discussion

A. Experimental setup

We train EfficientNet-B3 on UAV RGB canopy tiles (N=2,842) from four classes (*Healthy*, *Mosaic*, *PestAttack*, *Rust*) using a stratified train/val/test split. The fusion model concatenates the image embedding with z-scored numeric cues (ExG/VARI mean/std, luminance, blur, and leaf-area prior) and is optimized with AdamW, class reweighting, and a weighted sampler. Test-time inference uses resize and center crop without augmentation.

B. Detection performance (primary objective)

The RGB only baseline achieves macro-F1 $\approx$ 0.94, while hybrid late fusion improves macro-F1 to **0.98**, with strong per-class F1 for *Healthy/Mosaic/PestAttack/Rust* of 0.99/0.97/0.98/0.97, respectively. The largest gain is for *Rust*, where recall improves from $\sim$ 0.88 (RGB only) to $\sim$ 0.95 (fusion), indicating improved robustness to illumination and background variation. Fig. 4 shows sparse errors; most remaining confusion is between *Mosaic* and *PestAttack*, which can appear visually similar at canopy scale. We further visualize feature separability using a 2D t-SNE projection of the fused embeddings (Fig. 3). The four classes form compact, well-separated clusters, with slightly higher spread for *Rust*, which is consistent with its higher intra-class appearance variation under illumination and background changes.

C. Ablation: fusion vs. RGB only

Table II quantifies the contribution of numeric cues by comparing the full late-fusion model against an RGB only EfficientNet baseline. Removing numeric cues (i.e., training a

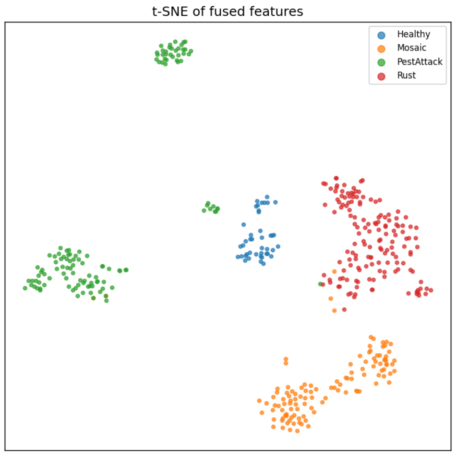

Fig. 3: t-SNE of fused features on the test set. Compact clusters indicate good class separability; *Rust* shows slightly larger spread due to higher visual variability.

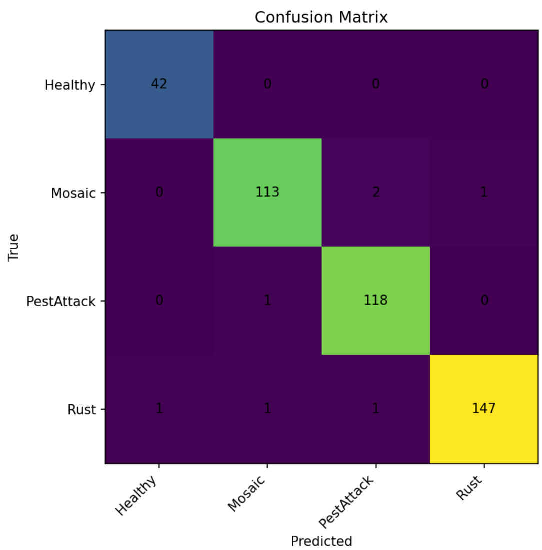

Fig. 4: Row-normalized confusion matrix on the test set (fusion). Errors are sparse; the main residual confusion is between *Mosaic* and *PestAttack*.

classifier on the EfficientNet embedding alone) reduces macro-F1 from 0.98 to $\sim$ 0.94, with the largest drop observed in *Rust* recall. This suggests that the added cues provide complementary, low-variance signals such as chromaticity, exposure, focus (blur), and canopy coverage that help disambiguate subtle symptoms and suppress spurious illumination effects. Overall, the ablation indicates that the performance gains are not solely due to the CNN backbone, but arise from the robustness added by fusing interpretable agronomic priors.

D. Action-level evaluation (secondary objective)

We convert recognition into actions using an RGB only severity proxy $\widehat{s}$ (affected leaf fraction within a leaf mask) and the score $S = \hat{p}_{\text{pred}}\widehat{s}$, with per-class thresholds $(p_{\min}, \tau_{\text{sev}})$ (Algorithm. 1, Algorithm. 2). Fig. 5 shows the SPRAY vs. NO-SPRAY confusion matrix using conservative defaults, which

TABLE II: Test-set detection (F1). Fusion adds 11 numeric indices to the EfficientNet-B3 embedding.

Model	Macro-F1	Healthy	Mosaic	PestAttack	Rust
EffNet-B3 (RGB)	0.94	0.99	0.97	0.97	0.88
Fusion (RGB+num)	**0.98**	**0.99**	**0.97**	**0.98**	**0.97**

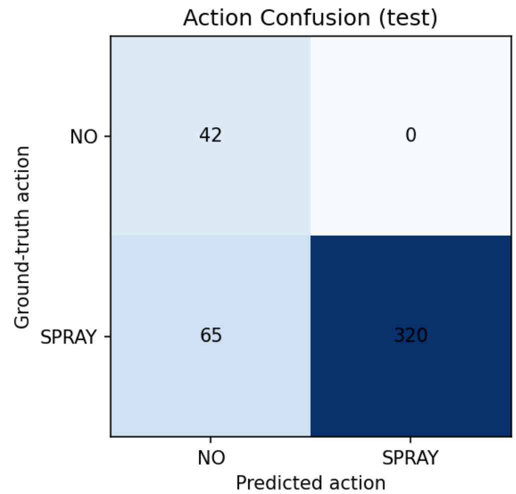

Fig. 5: Action confusion (SPRAY vs. NO-SPRAY) with conservative thresholds. No false sprays on *Healthy*; some diseased tiles are missed.

yields SPRAY precision $= 1.00$ and recall ≈ 0.83 (Table III). This operating point avoids over-spraying on *Healthy* tiles while capturing most diseased cases; thresholds can be tuned on validation to trade recall vs. over-spray risk.

E. Qualitative overlays

Fig. 6 provides representative overlays where the severity proxy highlights affected regions inside the leaf mask for *Rust*, *Mosaic*, and *PestAttack*. The MONITOR band acts as a safeguard for borderline cases (e.g., *Mosaic* under strong sunlight).

F. Spray/no-spray decision performance

Table III reports the binary action metrics at the default operating point. The model achieves perfect SPRAY precision (no false sprays) with recall $\approx$ 0.83, indicating that a conservative threshold avoids unnecessary chemical application while missing a subset of diseased tiles. If higher coverage is required, validation-tuned thresholds (or asymmetric costs) can increase SPRAY recall at the expense of some precision.

V. Conclusion and Future Work

This paper presented a hybrid late fusion framework for soybean disease detection and spray decision support using low cost UAV RGB imagery. By combining EfficientNet-B3 visual features with lightweight numeric cues, the proposed method achieved strong classification performance across four canopy classes and supported practical SPRAY, MONITOR, and NO-SPRAY recommendations through an RGBbased severity

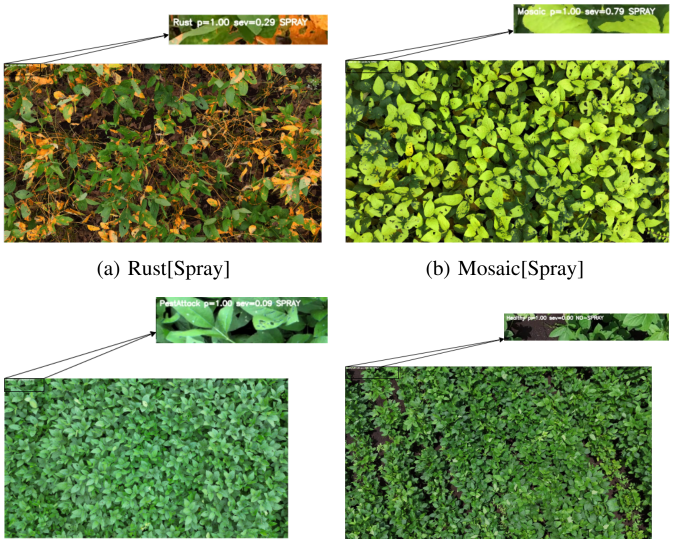

(a) Rust[Spray] (b) Mosaic[Spray]

(c) PestAttack[Spray] (d) Healthy[No-Spray]

Fig. 6: Severity overlays with predicted class, confidence, estimated severity, and recommended action. Colored pixels indicate the RGB proxy severity inside the leaf mask.

TABLE III: Binary spray decision performance on the test set (default decision threshold).

Class	precision	recall	f1-score	support
NO-SPRAY	0.393	1.000	0.564	42.000
SPRAY	1.000	0.831	0.908	385.000
accuracy		0.848		427.000
macro avg	0.696	0.916	0.736	427.000
weighted avg	0.940	0.848	0.874	427.000

proxy. A limitation of the current study is that evaluation was conducted on a relatively modest dataset collected under limited acquisition conditions. Future work will focus on broader validation across multiple seasons and locations, along with further assessment of the severity proxy against expert agronomic annotations.

Acknowledgment

The authors acknowledge the financial support from AgriHub: Innovation Hub for Agriculture, IIT Indore, funded by the Ministry of Electronics and Information Technology (MeitY), Government of India, under Project No. IIT/AgriHub/2025/PRJ-R/1.

References

[1] F. Lin, S. S. Chhapekar, C. C. Vieira, M. P. d. Silva, A. Rojas, D. Lee, N. Liu, E. M. Pardo, Y.-C. Lee, Z. Dong, J. B. Pinheiro, L. D. Ploper, J. Rupe, P. Chen, D. Wang, and H. T. Nguyen, "Breeding for disease resistance in soybean: A global perspective," *Theoretical and Applied Genetics*, vol. 135, no. 11, pp. 3773–3872, 2022.

[2] A. Mukherjee, S. Misra, and N. S. Raghuwanshi, "A survey of unmanned aerial sensing solutions in precision agriculture," *Journal of Network and Computer Applications*, vol. 148, p. 102461, 2019.

[3] J. Abdulridha, Y. Ampatzidis, J. Qureshi, and P. Roberts, "Laboratory and UAV-based identification and classification of tomato yellow leaf curl, bacterial spot, and target spot diseases in tomato utilizing hyperspectral imaging and machine learning," *Remote Sensing*, vol. 12, no. 17, p. 2732, 2020.

[4] H. Feng, H. Tao, Z. Li, G. Yang, and C. Zhao, "Comparison of UAV RGB imagery and hyperspectral remote-sensing data for monitoring winter wheat growth," *Remote Sensing*, vol. 14, no. 15, p. 3811, 2022.

[5] S. P. Mohanty, D. P. Hughes, and M. Salathé, "Using deep learning for image-based plant disease detection," *Frontiers in Plant Science*, vol. 7, p. 1419, 2016.

[6] K. P. Ferentinos, "Deep learning models for plant disease detection and diagnosis," *Computers and Electronics in Agriculture*, vol. 145, pp. 311–318, 2018.

[7] E. C. Tetila, B. B. Machado, G. K. Menezes, A. d. S. Oliveira Junior, M. A. Alvarez, W. P. Amorim, N. A. d. S. Belete, G. G. d. Silva, and H. Pistori, "Automatic recognition of soybean leaf diseases using UAV images and deep convolutional neural networks," *IEEE Geoscience and Remote Sensing Letters*, vol. 17, no. 5, pp. 903–907, 2020.

[8] S. Shinde and V. Attar, "An indian UAV and leaf image dataset for integrated crop health assessment of soybean crop," *Data in Brief*, vol. 60, p. 111517, 2025.

[9] N. Hussain, A. A. Farooque, A. W. Schumann, A. McKenzie-Gopsill, T. Esau, F. Abbas, B. Acharya, and Q. Zaman, "Design and development of a smart variable rate sprayer using deep learning," *Remote Sensing*, vol. 12, no. 24, p. 4091, 2020.

[10] A. A. Farooque, N. Hussain, A. W. Schumann, F. Abbas, H. Afzaal, A. McKenzie-Gopsill, T. Esau, Q. Zaman, and X. Wang, "Field evaluation of a deep learning-based smart variable-rate sprayer for targeted application of agrochemicals," *Smart Agricultural Technology*, vol. 3, p. 100073, 2023.

[11] M. Tan and Q. V. Le, "EfficientNet: Rethinking model scaling for convolutional neural networks," in *Proceedings of the 36th International Conference on Machine Learning (ICML)*, 2019, pp. 6105–6114.

[12] D. M. Woebbecke, G. E. Meyer, K. Von Bargen, and D. A. Mortensen, "Color indices for weed identification under various soil, residue, and lighting conditions," *Transactions of the ASAE*, vol. 38, no. 1, pp. 259–269, 1995.

[13] A. A. Gitelson, Y. J. Kaufman, R. Stark, and D. Rundquist, "Novel algorithms for remote estimation of vegetation fraction," *Remote Sensing of Environment*, vol. 80, no. 1, pp. 76–87, 2002.

[14] R. M. Haralick, K. Shanmugam, and I. Dinstein, "Textural features for image classification," *IEEE Transactions on Systems, Man, and Cybernetics*, vol. SMC-3, no. 6, pp. 610–621, 1973.

[15] E. C. Tetila, B. B. Machado, N. A. d. S. Belete, D. A. Guimaraes, and H. Pistori, "Identification of soybean foliar diseases using unmanned aerial vehicle images," *IEEE Geoscience and Remote Sensing Letters*, vol. 14, no. 12, pp. 2190–2194, 2017.

[16] E. C. Tetila, B. B. Machado, G. Astolfi, N. A. d. S. Belete, W. P. Amorim, A. R. Roel, and H. Pistori, "Detection and classification of soybean pests using deep learning with UAV images," *Computers and Electronics in Agriculture*, vol. 179, p. 105836, 2020.

[17] M. J. A. Soeb, M. F. Jubayer, T. A. Tarin, M. R. Al Mamun, F. M. Ruhad, A. Parven, N. M. Mubarak, S. L. Karri, and I. M. Meftaul, "Tea leaf disease detection and identification based on YOLOv7 (YOLO-T)," *Scientific Reports*, vol. 13, p. 6078, 2023.

[18] W. Bao, T. Fan, G. Hu, D. Liang, and H. Li, "Detection and identification of tea leaf diseases based on AX-RetinaNet," *Scientific Reports*, vol. 12, p. 2183, 2022.

[19] T. Zhang, Z. Xu, J. Su, Z. Yang, C. Liu, W.-H. Chen, and J. Li, "Ir-UNet: Irregular segmentation u-shape network for wheat yellow rust detection by UAV multispectral imagery," *Remote Sensing*, vol. 13, no. 19, p. 3892, 2021.

[20] Y. Lyu, X. Han, P. Wang, J.-Y. Shin, and M.-W. Ju, "Unmanned aerial vehicle-based RGB imaging and lightweight deep learning for downy mildew detection in kimchi cabbage," *Remote Sensing*, vol. 17, no. 14, p. 2388, 2025.

[21] A. Mahmood, W. Anwar, H. Sattar, S. R. Hassan, M. Sheraz, T. C. Chuah *et al.*, "Deep learning framework using UAV imagery for multi-disease detection in cereal crops," *Scientific Reports*, vol. 16, p. 3339, 2026.